JACS
JOURNAL OF THE AMERICAN CHEMICAL SOCIETY
Communication
pubs.acs.org/JACS

Synthesis, Characterization, and Nonvolatile Ternary Memory Behavior of a Larger Heteroacene with Nine Linearly Fused Rings and Two Different Heteroatoms

Pei-Yang Gu,[†,‡] Feng Zhou,[†] Junkuo Gao,[‡] Gang Li,[‡] Chengyuan Wang,[‡] Qing-Feng Xu,[†] Qichun Zhang,*[,‡] and Jian-Mei Lu*[,†]

[†]College of Chemistry, Chemical Engineering and Materials Science, Soochow University, Suzhou, 215123, China

[‡]School of Materials Science and Engineering, Nanyang Technological University, Singapore 639798, Singapore

Supporting Information

ABSTRACT: To achieve ultrahigh density memory devices with the capacity of 3^n or larger, organic materials with multilevel stable states are highly desirable. Here, we reported a novel larger stable heteroacene, 2,3,13,14-tetradecyloxy-5,11,16,22-tetraaza-6,10,17,21-tetrachloro-7,9,18,20-tetraoxa-8,19-dicyanoenneacene (CDPzN), which has two different types of heteroatoms (O and N) and nine linearly fused rings. The sandwich-structure memory devices based on CDPzN exhibited excellent ternary memory behaviors with high ON2/ON1/OFF current ratios of $10^{6.3}/10^{4.3}/1$ and good stability for these three states.

The exponential growth of information communication poses a strong demand for developing next-generation memory devices with high-density data storage, low cost, simple structure, fast speed, lower power consumption, and longer data retention time.[1] Clearly, traditional inorganic-semiconductor-based systems have reached their bottle necks and face big challenges to further enhance their memory capacities.[2] Recently, organic memory devices have evoked a lot of research interest because they could realize ultrahigh density data storage through either a 3D-stacked cross-bar array or multilevel stable oxidation states.[3] Currently, most resistive organic memory devices are based on binary materials, which have two conductivity states [i.e., ON ("1", high conductivity) and OFF ("0", low conductivity) states] in response to the applied voltage.[4] Such devices only can store 2-bits in a single cell. Thus, in order to achieve ultrahigh density memory devices, organic materials with multilevel stable states, which can lead to an increasing capacity of 3^n or larger, are highly desirable.[5]

Among all organic materials for data storage, small organic molecules are more promising in approaching high-performance data storage because of their tunable properties and designable structures.[6] Although some molecules have been demonstrated to show "0", "1", and "2" tristable states and could store more than 2-bits in a single cell, such systems are still rare and it is still desirable to search new organic compounds with a reliable storage capacity of 3^n or larger.[7]

Oligoacenes have been widely used as active layers in organic semiconductor devices such as organic field-effect transistors, organic light emitting diodes, organic solar cells, or even memory devices.[8] Yet, they have stability issues due to photo-oxidation or dimerization *via* a Diels−Alder reaction. Such problems could be solved through the replacement of CH groups in the backbone of oligoacenes with heteroatoms (e.g., N, O, P, B, S).[9] In fact, the type/position/number of heteroatoms will offer us more chances to tune the highest occupied molecular orbital (HOMO)−lowest unoccupied molecular orbital (LUMO) gap, HOMO/LUMO positions, and the stability of as-prepared oligoheteroacenes.[10] In past decades, significant advancements have been witnessed in synthesis, theoretical study, and applications of heteroacenes.[11]

In this report, we are interested in larger heteroacenes with two or more different types of heteroatoms because (1) more heteroatoms might provide multilevel stable oxidation states, which is very important to realize 3^n or larger data storage; (2) synthetic work should be more challenging; and (3) we will have more chances to tune the stability and properties of as-designed molecules. We reported here a novel larger heteroacene (2,3,13,14-tetradecyloxy-5,11,16,22-tetraaza-6,10,17,21-tetrachloro-7,9,18,20-tetraoxa-8,19-dicyanoenneacene, abbreviated as CDPzN, **1**), which has two different types of heteroatoms (O and N) and nine linearly fused rings. We believe that CDPzN should have the following advantages: (1) the introduction of an O atom could make CDPzN more stable in both the ground and oxidation state; (2) the cyano group may be useful for negative charge injection as suggested in previous reports;[12] and (3) the memory device based on CDPzN might exhibit multilevel stable conductivity states in response to the applied voltage because the electron-withdrawing abilities of cyano and pyrazine are different.

The synthetic route for the preparation of CDPzN is described in Scheme 1. The target compound was synthesized in two steps: first, the commercially available chloranilic acid was reacted with 1,2-bis(decyloxy)-4,5-diaminobenzene (0.9 equiv) in ethylalcohol to afford 1,4-dichloro-7,8-bis(decyloxy)-phenazine-2,3-diol (**2**) in 55% yield. Then the as-prepared intermediate **2** was condensed with tetrafluoroterephthalonitrile (0.45 equiv) using potassium carbonate (5 equiv) as the base to generate CDPzN in 85% yield.

Received: August 8, 2013
Published: September 11, 2013

ACS Publications © 2013 American Chemical Society

dx.doi.org/10.1021/ja408208c | J. Am. Chem. Soc. 2013, 135, 14086−14089

Scheme 1. Synthetic Route of CDPzN[a]

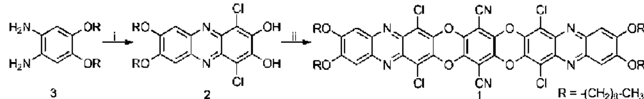

[a](i) 1.1 equiv of chloranilic acid, CH_3CH_2OH, N_2, reflux, 55%; (ii) 0.45 equiv of tetrafluoroterephthalonitrile, 5 equiv of K_2CO_3, DMF, 100 °C, 85%.

The optical, thermal, and electrochemical properties of CDPzN have been studied. Figure 1a shows the normalized optical absorption spectrum of the CDPzN thin film on a quartz plate. The absorption spectrum of CDPzN exhibits three prominent bands at 233, 266, and 379 nm, which can be ascribed to a localized aromatic $\pi-\pi^*$ transition and intramolecular charge transfer from the donor (decyloxy) to the acceptor (pyrazine and cyano) moieties, respectively. CDPzN exhibits a very good thermal stability, with an onset decomposition temperature of ~367 °C (considering the 5% weight loss temperature, Figure S6). The excellent thermal property of CDPzN is expected to meet the requirements of heat resistance in the electronics industry.

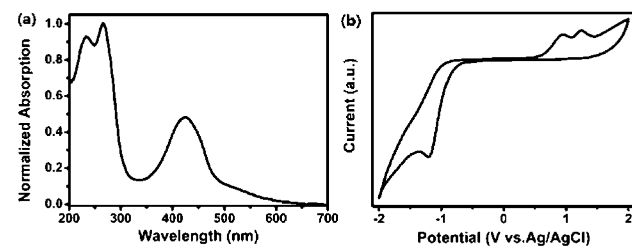

Figure 1. Characterization of CDPzN. (a) Normalized optical absorption spectra of CDPzN thin film on a quartz plate. (b) Cyclic voltammogram curve of CDPzN thin films on ITO glass in a 0.1 M solution of $TBAPF_6$ in acetonitrile solution. The scan rate: 100 mV s^{-1}.

Figure 1b shows the cyclic voltammogram (CV) curve of the CDPzN film on an indium–tin oxide (ITO) glass substrate in a 0.1 mol L^{-1} solution of tetrabutylammonium hexafluorophosphate ($TBAPF_6$) in anhydrous acetonitrile solution. The onset reduction and oxidation potentials for CDPZN are −1.22, 0.94, and 1.24 V, which correspond to the LUMO, HOMO, and HOMO-1 energy levels of ~ −3.20, −5.34, and −5.64 eV using the equation $E_{LUMO/HOMO} = -e\ (4.40 + E_{red/oxd}^{onset})$ eV.[13] The calculated band gap using CV data is 2.10 eV for CDPzN, which was slightly smaller compared to the optical onset-edge band gap result (2.43 eV).

Figure 2a shows the scheme of our prototype memory device, which is a sandwich structure using ITO as bottom electrodes, aluminum (Al, 100 nm thickness) as top electrodes, and an organic layer of CDPzN molecules as an active layer. The film thickness was about 100 nm, as measured by SEM through a cross section of the film (Figure 2a).

The current–voltage ($I-V$) characteristics of the device were measured by an HP4145B semiconductor parameter analyzer. Figure 2b shows the typical $I-V$ curve of a CDPzN-based memory device. In the first sweep from 0 to −4 V, two sharp transitions from the low-conductivity (OFF, "0") state to an intermediate-conductivity (ON1, "1") state, to a high-conductivity (ON2, "2") state were observed at switching threshold voltages (STVs) of −2.43 and −3.31 V, respectively.

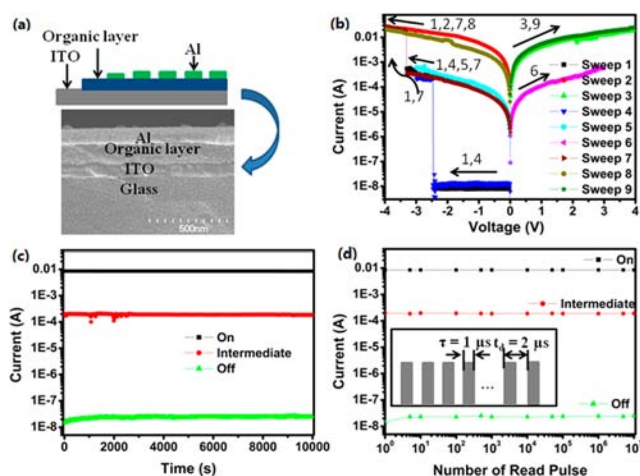

Figure 2. Memory-device characteristics of CDPzN. (a) Scheme of the sandwich device and SEM image of a cross section of the device. (b) $I-V$ characteristics of the memory device fabricated with CDPzN. (c) Stability of the device in three states under a constant "read" voltage of −1 V. (d) Stimulus effect of read pulse of −1 V on the ON, intermediate, and OFF states. Inset shows the pulse shapes of the measurements.

These OFF-to-ON1 and ON1-to-ON2 transitions can be regarded as a "writing" process. For the subsequent negative sweep from 0 to −4 V (sweep 2) and the positive sweep from 0 to 4 V (sweep 3), the storage cell of the device maintains the ON state. Another cell of the device was measured over a voltage range of 0 to −3 V (sweep 4) and showed one STV at −2.48 V, which suggested that this cell was switched from the OFF state to the ON1 state. For the subsequent negative sweep from 0 to −3 V (sweep 5) and the reverse voltage sweep (sweep 6), the current density maintains the ON1 state. This result indicated that once the cell reached the ON1 state, it could still be maintained even when the power was shut off. The storage cell underwent a transition from the ON1 to ON2 state at 3.31 V for the subsequent negative sweep from 0 to −4 V (sweep 7). Once it was switched to the ON2 state, the memory device cannot return back to both the ON1 and OFF states (sweeps 8–9). The three states of the ternary memory cell are distinct, and the current ratio of the "OFF", "ON1", and "ON2" states is $1{:}10^{4.3}{:}10^{6.3}$. This device exhibits a typical write-once read-many-times (WORM) behavior.

Figure 2c shows the retention times and stress tests of the memory device for the OFF, ON1, and ON2 states. Under a constant stress of −1 V, no significant degradation in current for three different states could be observed for at least 10 000 s during the readout test. Moreover, the stimulus effect of continuous read pulses of −1 V on the three different states was also investigated. As shown in Figure 2d (inset), the pulse period and pulse width are 2 and 1 μs, respectively, which are typical values in practical devices. The three different states in memory devices are stable for at least 10^7 continuous read cycles. Therefore, the switching behavior on the remnant stored data and the nonvolatile nature of the memory device can explain the functionality of a WORM-type memory characteristic.

In order to understand the electrical switching behavior of the CDPzN memory device, theoretical calculations have been performed using the density functional theory (DFT) method of B3LYP with the 6-31G (d) basis set.[14] Figure 3a, 3b show that the electron density distributions of the HOMO mainly

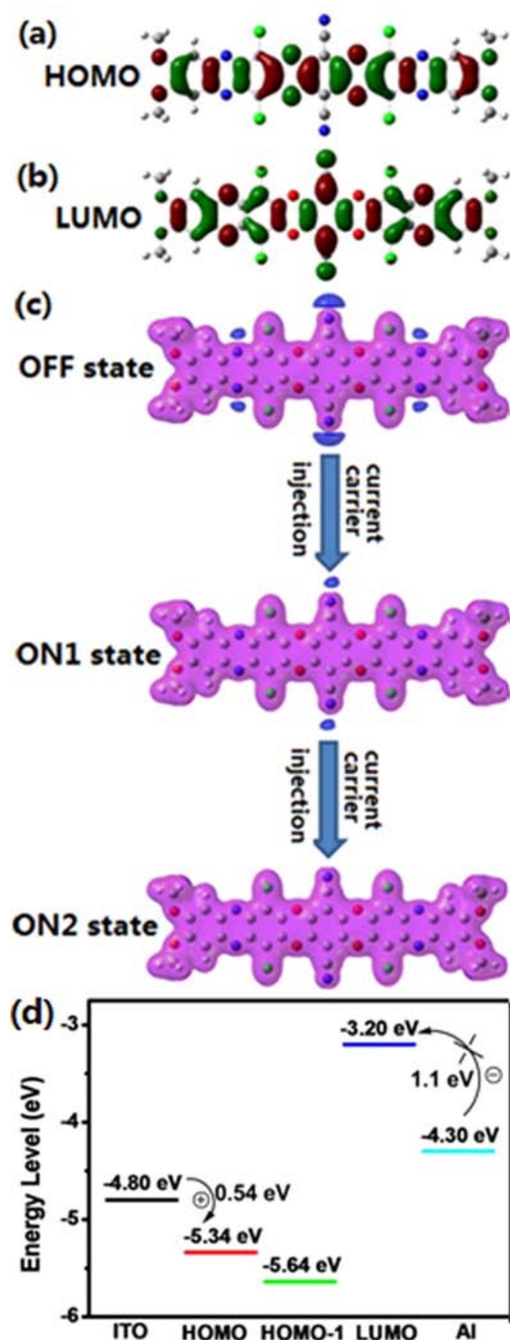

Figure 3. DFT molecular simulation results and energy level diagram. (a, b) HOMO and LUMO of CDPzN. (c) Possible carriers' migration process based on ITO/CDPzN/Al devices. (d) Energy level diagram of HOMO, HOMO-1, and LUMO for CDPzN along with the work function of the electrodes.

locate on aromatic groups while the LUMO orbital is mainly distributed on both pyrazine and cyano groups. Generally, the conjugated molecules with such electron distribution indicate the intramolecular charge transfer (ICT) property. Upon undergoing the HOMO to LUMO transition, the trend of the distribution on electron density displays two ways: one way is a shift from the aromatic groups to the pyrazine groups, and the other way is to move from the aromatic groups to the cyano groups, which implies that the memory device based on this molecule could exhibit two switching threshold voltages (STVs), which is consistent with the experimental results. Figure 3c (OFF state) shows that the molecular surface has continuous positive electrostatic potential (in red) along the conjugated backbone, indicating that charge carriers can migrate through this open channel. However, there are some negative electrostatic potential regions (in blue) caused by electron-acceptor groups. These negative regions can serve as "charge traps" to block the mobility of charge carriers. As shown in Figure 3d, the energy barrier (0.54 eV) between the work function of ITO (−4.8 eV) and HOMO (−5.34 eV, calculation based on CV) is lower than the energy barrier (1.1 eV) between the work functions of Al (−4.3 eV) and LUMO (−3.20 eV). Thus, holes might dominate the conduction process in ITO/CDPzN/Al devices. The atomic force microscopy (AFM) image (Figure S7) shows that the film is smooth with good quality, which indicates that two charge traps (pyrazine and cyano groups) have equal opportunities to accept the injected charge carriers. Possible charge carrier migration processes are proposed in Figure 3c. Under low bias, the CDPzN thin film is in a low-conductivity (OFF) state because the energy barrier between the Al electrode and the CDPzN layer is as large as 1.1 eV, which also blocks the electron migration. Under high bias, the hole injection is easier and the CDPzN has better conductivity at the intermediate-conductivity (ON1) state, which corresponds to the first oxidation process. However, two traps are not filled at the same time: the trap of pyrazine is filled and the trap of cyano is partly filled, which could be attributed to the stronger electron-withdrawing ability of cyano than pyrazine. With increasing bias, the trap of cyano is also filled which leads to the current transition from the ON1 to ON2 state, which corresponds to the second oxidation process. Consequently, the device shows multilevel memory characteristics due to the two charge traps with the different electron-withdrawing abilities of cyano and pyrazine.

In summary, we have successfully synthesized a novel larger stable heteroacene, CDPzN, containing two different types of heteroatoms (N and O atoms) in their backbones and having nine linearly fused rings. The sandwich-structure memory devices based on CDPzN exhibited excellent ternary memory behavior with high ON2/ON1/OFF current ratios of $10^{6.3}$/$10^{4.3}$/1 and good stability for the three states. We believe that our results could provide guidance for the design and synthesis of new heteroacenes, which could be used as promising candidates in nonvolatile memory devices.

■ ASSOCIATED CONTENT

Ⓢ Supporting Information

Experimental procedures, synthesis of CDPzN, fabrication and measurements of the memory devices. This material is available free of charge via the Internet at http://pubs.acs.org.

■ AUTHOR INFORMATION

Corresponding Authors

qczhang@ntu.edu.sg
lujm@suda.edu.cn

Notes

The authors declare no competing financial interest.

■ ACKNOWLEDGMENTS

The work is supported by the Singapore National Research Foundation through the Competitive Research Programme under Project No. NRF-CRP5-2009-04 (J.G., Y.Z., and C.X.). Q.Z. acknowledges the financial support AcRF Tier 1 (RG 16/

12) and Tier 2 (ARC 20/12 and ARC 2/13) from MOE, CREATE program (Nanomaterials for Energy and Water Management) from NRF, and New Initiative Fund from NTU, Singapore. P.-Y. Gu thanks the China Scholarship Council (CSC).

REFERENCES

(1) (a) Moller, S.; Perlov, C.; Jackson, W.; Taussig, C.; Forrest, S. R. *Nature* **2003**, *426*, 166−169. (b) Ling, Q.-D.; Liaw, D.-J.; Zhu, C.; Chan, D. S.-H.; Kang, E.-T.; Neoh, K.-G. *Prog. Polym. Sci.* **2008**, *33*, 917−978. (c) Scott, J. C.; Bozano, L. D. *Adv. Mater.* **2007**, *19*, 1452−1463.

(2) (a) Lu, W.; Lieber, C. M. *Nat. Mater.* **2007**, *6*, 841−850. (b) Jung, Y.; Lee, S.-H.; Jennings, A. T.; Agarwal, R. *Nano Lett.* **2008**, *8*, 2056−2062.

(3) (a) Liu, G.; Ling, Q.-D.; Teo, E. Y. H.; Zhu, C.-X.; Chan, D. S.-H.; Neoh, K.-G.; Kang, E.-T. *ACS Nano* **2009**, *3*, 1929−1937. (b) Simão, C.; Mas-Torrent, M.; Casado-Montenegro, J.; Otón, F.; Veciana, J.; Rovira, C. *J. Am. Chem. Soc.* **2011**, *133*, 13256−13259.

(4) (a) Kapetanakis, E.; Douvas, A. M.; Velessiotis, D.; Makarona, E.; Argitis, P.; Glezos, N.; Normand, P. *Adv. Mater.* **2008**, *20*, 4568−4574. (b) Chu, C. W.; Ouyang, J.; Tseng, J.-H.; Yang, Y. *Adv. Mater.* **2005**, *17*, 1440−1443. (c) Tseng, R. J.; Huang, J.; Ouyang, J.; Kaner, R. B.; Yang, Y. *Nano Lett.* **2005**, *5*, 1077−1080. (d) Ouyang, J.; Chu, C.-W.; Szmanda, C. R.; Ma, L.; Yang, Y. *Nat. Mater.* **2004**, *3*, 918−922. (f) Bozano, L. D.; Kean, B. W.; Beinhoff, M.; Carter, K. R.; Rice, P. M.; Scott, J. C. *Adv. Funct. Mater.* **2005**, *15*, 1933−1939.

(5) (a) Lee, J.-S.; Kim, Y.-M.; Kwon, J.-H.; Sim, J. S.; Shin, H.; Sohn, B.-H.; Jia, Q. *Adv. Mater.* **2011**, *23*, 2064−2068. (b) Liu, S.-J.; Wang, P.; Zhao, Q.; Yang, H.-Y.; Wong, J.; Sun, H.-B; Dong, X.-C.; Lin, W.-P.; Huang, W. *Adv. Mater.* **2012**, *24*, 2901−2905. (c) Ye, C.; Peng, Q.; Li, M.; Luo, J.; Tang, Z.; Pei, J.; Chen, J.; Shuai, Z.; Jiang, L.; Song, Y. *J. Am. Chem. Soc.* **2012**, *134*, 20053−20059. (d) Li, H.; Xu, Q.; Li, N.; Sun, R.; Ge, J.; Lu, J.; Gu, H.; Yan, F. *J. Am. Chem. Soc.* **2010**, *132*, 5542−5543.

(6) (a) Raymo, F. M. *Adv. Mater.* **2002**, *14*, 401−414. (b) Rozenberg, M. J.; Inoue, I. H.; Sánchez, M. J. *Phys. Rev. Lett.* **2004**, *92*, 178302. (c) Naber, R. C. G.; Asadi, K.; Blom, P. W. M.; de Leeuw, D. M.; De Boer, B. *Adv. Mater.* **2010**, *22*, 933−945. (d) Li, G.; Zheng, K.; Wang, C.; Leck, K. S.; Hu, F.; Sun, X. W.; Zhang, Q. *ACS Appl. Mater. Interfaces* **2013**, *5*, 6458−6462. (e) Miao, S.; Li, H.; Xu, Q.; Li, N.; Zheng, J.; Sun, R.; Lu, J.; Li, C. M. *J. Mater. Chem.* **2012**, *22*, 16582−16589.

(7) (a) Kronemeijer, A. J.; Akkerman, H. B.; Kudernac, T.; van Wees, B. J.; Feringa, B. L.; Blom, P. W. M.; de Boer, B. *Adv. Mater.* **2008**, *20*, 1467−1473. (b) Wang, J.; Stucky, G. D. *Adv. Funct. Mater.* **2004**, *14*, 409−415. (c) Lee, T.; Kim, S.-U.; Min, J.; Choi, J.-W. *Adv. Mater.* **2010**, *22*, 510−514.

(8) (a) Herwig, P. T.; Müllen, K. *Adv. Mater.* **1999**, *11*, 480−483. (b) Giri, G.; Verploegen, E.; Mannsfeld, S. C. B.; Atahan-Evrenk, S.; Kim, D. H.; Lee, S. Y.; Becerril, H. A.; Aspuru-Guzik, A.; Toney, M. F.; Bao, Z. *Nature* **2011**, *480*, 504−508. (c) Murphy, A. R.; Fréchet, J. M. J. *Chem. Rev.* **2007**, *107*, 1066−1096. (d) Li, J.; Zhang, Q. *Synlett* **2013**, *24*, 686−696. (e) Payne, M. M.; Parkin, S. R.; Anthony, J. E. *J. Am. Chem. Soc.* **2005**, *127*, 8028−8029. (f) Xiao, J.; Divayana, Y.; Zhang, Q.; Doung, H. M.; Zhang, H.; Boey, F.; Sun, X. W.; Wudl, F. *J. Mater. Chem.* **2010**, *20*, 8167−8170. (g) Qu, H.; Chi, C. A *Org. Lett.* **2010**, *12*, 3360−3363. (h) Zhang, Q.; Divayana, Y.; Xiao, J.; Wang, Z.; Tiekink, E. R. T.; Doung, H. M.; Zhang, H.; Boey, F.; Sun, X. W.; Wudl, F. *Chem.—Eur. J.* **2010**, *16*, 7422−7426. (i) Xiao, J.; Duong, H. M.; Liu, Y.; Shi, W.; Ji, L.; Li, G.; Li, S.; Liu, X.-W.; Ma, J.; Wudl, F.; Zhang, Q. *Angew. Chem., Int. Ed.* **2012**, *51*, 6094−6098. (j) Xiao, J.; Liu, S.; Liu, Y.; Ji, L.; Liu, X.; Zhang, H.; Sun, X.; Zhang, Q. *Chem.—Asian J.* **2012**, *7*, 561−564.

(9) (a) Miao, S.; Brombosz, S. M.; Schleyer, P. V. R.; Wu, J. I.; Barlow, S.; Marder, S. R.; Hardcastle, K. I.; Bunz, U. H. F. *J. Am. Chem. Soc.* **2008**, *130*, 7339−7344. (b) Li, G.; Wu, Y.; Gao, J.; Wang, C.; Li, J.; Zhang, H.; Zhao, Y.; Zhao, Y.; Zhang, Q. *J. Am. Chem. Soc.* **2012**, *134*, 20298−20301. (c) Liang, Z.; Tang, Q.; Xu, J.; Miao, Q. *Adv. Mater.* **2011**, *23*, 1535−1539. (d) Li, G.; Wu, Y.; Gao, J.; Li, J.; Zhao, Y.; Zhang, Q. *Chem.—Asian J.* **2013**, *8*, 1574−1578. (e) Seillan, C.; Brisset, H.; Siri, O. *Org. Lett.* **2008**, *10*, 4013−4016. (f) Li, G.; Duong, H. M.; Zhang, Z.; Xiao, J.; Liu, L.; Zhao, Y.; Zhang, H.; Huo, F.; Li, S.; Ma, J.; Wudl, F.; Zhang, Q. *Chem. Commun.* **2012**, *48*, 5974−5976. (g) McGrath; Kelly, K.; Jang, K.; Robins; Kathleen, A.; Lee, D.-C. *Chem.—Eur. J.* **2009**, *15*, 4070−4077. (h) Wu, Y.; Yin, Z.; Xiao, J.; Liu, Y.; Wei, F.; Tan, K. J.; Kloc, C.; Huang, L.; Yan, Q.; Hu, F.; Zhang, H.; Zhang, Q. *ACS Appl. Mater. Interfaces* **2012**, *4*, 1883−1886. (i) Takimiya, K.; Shinamura, S.; Osaka, I.; Miyazaki, E. *Adv. Mater.* **2011**, *23*, 4347−4370. (j) Gao, B.; Wang, M.; Cheng, Y.; Wang, L.; Jing, X.; Wang, F. *J. Am. Chem. Soc.* **2008**, *130*, 8297−8306.

(10) (a) Sokolov, A. N.; Atahan-Evrenk, S.; Mondal, R.; Akkerman, H. B.; Sánchez-Carrera, R. S.; Granados-Focil, S.; Schrier, J.; Mannsfeld, S. C. B.; Zoombelt, A. P.; Bao, Z.; Aspuru-Guzik, A. *Nat. Commun.* **2011**, *2*, 437. (b) Watanabe, M.; Chen, K.-Y.; Chang, Y. J.; Chow, T. J. *Acc. Chem. Res.* **2013**, *46*, 1606−1615. (c) Bunz, U. H. F.; Engelhart, J. U.; Lindner, B. D.; Schaffroth, M. *Angew. Chem., Int. Ed.* **2013**, *52*, 3810−3821.

(11) (a) Jiang, W.; Li, Y.; Wang, Z. *Chem. Soc. Rev.* **2013**, *42*, 6113−6127. (b) Richards, G. J.; Hill, J. P.; Mori, T.; Ariga, K. *Org. Biomol. Chem.* **2011**, *9*, 5005−5017. (c) Anthony, J. E. *Chem. Rev.* **2006**, *106*, 5028−5048.

(12) (a) Miao, S.; Zhu, Y.; Zhuang, H.; Xu, X.; Li, H.; Sun, R.; Li, N.; Ji, S.; Lu, J. *J. Mater. Chem. C* **2013**, *1*, 2320−2327. (b) Yang, Y.; Ouyang, J.; Ma, L.; Tseng, R. J.-H.; Chu, C.-W. *Adv. Funct. Mater.* **2006**, *16*, 1001−1014.

(13) Zhang, W.; Sun, X.; Xia, P.; Huang, J.; Yu, G.; Wong, M. S.; Liu, Y.; Zhu, D. *Org. Lett.* **2012**, *14*, 4382−4385.

(14) (a) Gu, P.-Y.; Lu, C.-J.; Hu, Z.-J.; Li, N.-J.; Zhao, T.-T.; Xu, Q.-F.; Xu, Q.-H.; Zhang, J.-D.; Lu, J.-M. *J. Mater. Chem. C* **2013**, *1*, 2599−2606. (b) Kim, S.; Zheng, Q. D.; He, G. S.; Bharali, D. J.; Pudavar, H. E.; Baev, A.; Prasad, P. N. *Adv. Funct. Mater.* **2006**, *16*, 2317−2323.